SCIENTIFIC REPORTS

OPEN

SUBJECT AREAS:
SPINTRONICS
APPLIED PHYSICS
MAGNETIC PROPERTIES AND MATERIALS

Received
15 May 2014

Accepted
9 December 2014

Published
12 January 2015

Correspondence and requests for materials should be addressed to T.R.A. (arslanovt@gmail.com) or S.L.-M. (Lsinhue@yahoo.com.mx)

Pressure control of magnetic clusters in strongly inhomogeneous ferromagnetic chalcopyrites

Temirlan R. Arslanov[1], Akhmedbek Yu. Mollaev[1], Ibragimkhan K. Kamilov[1], Rasul K. Arslanov[1], Lukasz Kilanski[2], Roman Minikaev[2], Anna Reszka[2], Sinhué López-Moreno[3], Aldo H. Romero[4], Muhammad Ramzan[5], Puspamitra Panigrahi[5,6], Rajeev Ahuja[5,6], Vladimir M. Trukhan[7], Tapan Chatterji[8], Sergey F. Marenkin[9] & Tatyana V. Shoukavaya[7]

[1]Amirkhanov Institute of Physics, Daghestan Scientific Center RAS 367003 Makhachkala, Russia, [2]Institute of Physics, Polish Academy of Sciences, Al. Lotnikow 32/46, 02-668 Warsaw, Poland, [3]Centro de Investigación en Corrosión, Universidad Autónoma de Campeche, Av. Herore de Nacozari 480, Campeche, Campeche 24029, México, [4]Physics Department, West Virginia University, Morgantown, 26506-6315 West Virginia, USA, [5]Department of Physics and Astronomy, Uppsala University, 75120 Uppsala, Sweden, [6]Department of Materials and Engineering, Royal Institute of Technology, 10044 Stockholm, Sweden, [7]Scientific-Practical Materials Research Centre (SSPA) of NAS of Belarus, 220072 Minsk, Belarus, [8]Institute Laue-Langevin, Boîte Postale 156, 38042 Grenoble Cedex 9, France, [9]Kurnakov Institute of General and Inorganic Chemistry RAS, 119991 Moscow, Russia.

Room-temperature ferromagnetism in Mn-doped chalcopyrites is a desire aspect when applying those materials to spin electronics. However, dominance of high Curie-temperatures due to cluster formation or inhomogeneities limited their consideration. Here we report how an external perturbation such as applied hydrostatic pressure in $CdGeP_2$:Mn induces a two serial magnetic transitions from ferromagnet to non-magnet state at room temperature. This effect is related to the unconventional properties of created MnP magnetic clusters within the host material. Such behavior is also discussed in connection with *ab initio* density functional calculations, where the structural properties of MnP indicate magnetic transitions as function of pressure as observed experimentally. Our results point out new ways to obtain controlled response of embedded magnetic clusters.

The rapid developments observed recently in the field of spintronics have generated the appearance of new related research topics[1], which are based on a variety of traditional or more novel materials such as graphene or topological insulators[2]. Among those new proposals, there is also the exploration of the current-induced spin transfer or thermal gradient induce spin current effects by using ferromagnetic semiconductors or diluted magnetic semiconductors (DMSs) as an alternative approach to control the system magnetization and the spin current[3–5]. These possibilities have encountered the problem of the operability at room temperature (RT), a common dilemma with other proposals. Although most of pure DMSs are good source of spin polarized carriers[6,7], their low ferromagnetic ordering temperature (T_C) is a serious shortcoming. Similarly, DMSs containing additional inclusions, such as metallic clusters and inhomogeneities are usually avoided because they add an uncontrolled mechanism of transport and magnetism. On the other hand, the presence of ferromagnetism in DMSs, with a magnetic moment value that depends on cluster size inclusions, shows notable T_C increase, which has been reported to be above RT[8,9]. Furthermore, their self-organization can open a promising path for magnetic recording media due to their large positive magnetoresistance[8]. In recent reports the possibility of spin polarization due to the presence of magnetic clusters within the sample is under debate[10,11]. Until now, however, no direct evidence on their impact to the magnetic response has been addressed and therefore the understanding of the role of the magnetic clusters into the magnetization in DMSs requires a different approach.

The clustering formation and presence of inhomogeneities are reported to have a direct influence in the high T_C in ferromagnetic chalcopyrite-based materials[12–18]. Recently, we have shown that the competing interplay between MnAs micro-size clusters in Mn-doped $CdGeAs_2$ lead to unusual pressure tunable metamagnet-like states[19]. The direct control of magnetic behavior of clusters via an external pressure in these inhomogeneous systems could lead to striking magnetic phenomena. In particular, among all high-T_C ferromagnetic chalcopyr-

ites, Mn-doped $CdGeP_2$[20] is a prototypical material, where the clusters influence on the magnetic response can be clearly characterized. However, consideration of an external pressure and its influence to the magnetic response of such systems has not been yet considered[21].

Here we report our first investigation of ferromagnetic MnP clusters in strongly inhomogeneous Mn-doped $CdGeP_2$, using systematic high-pressure measurements (magnetic, volume, and transport). We clearly identify, two RT serial transitions, starting from a ferromagnetic (FM) to non-magnetic (NM) state. We show below that this effect is coming from MnP cluster response to the external pressure. Specifically, for the low pressure regime, the results suggest that an enhancement in the stability of the host structure is highly realized as the concentration of Mn doping goes from $x = 0.09$ to $x = 0.25$, as can be seen on Fig. 1 b. For small Mn doping levels, the sample pressure response behaves mostly as the undoped host. While at large doping levels, the magnetic response is largely tuned by the presence of MnP clusters, which have been observed at ambient pressure. To offer a light into our magnetic and volume measurements, we correlate the observed cluster changes with theoretical density functional theory (DFT) calculations. In particular we study the pressure-volume dependence of single orthorhombic MnP crystal as well as the effect of substitutional Mn in the magnetic and structural properties of $Cd_{1-x}Mn_xGeP_2$.

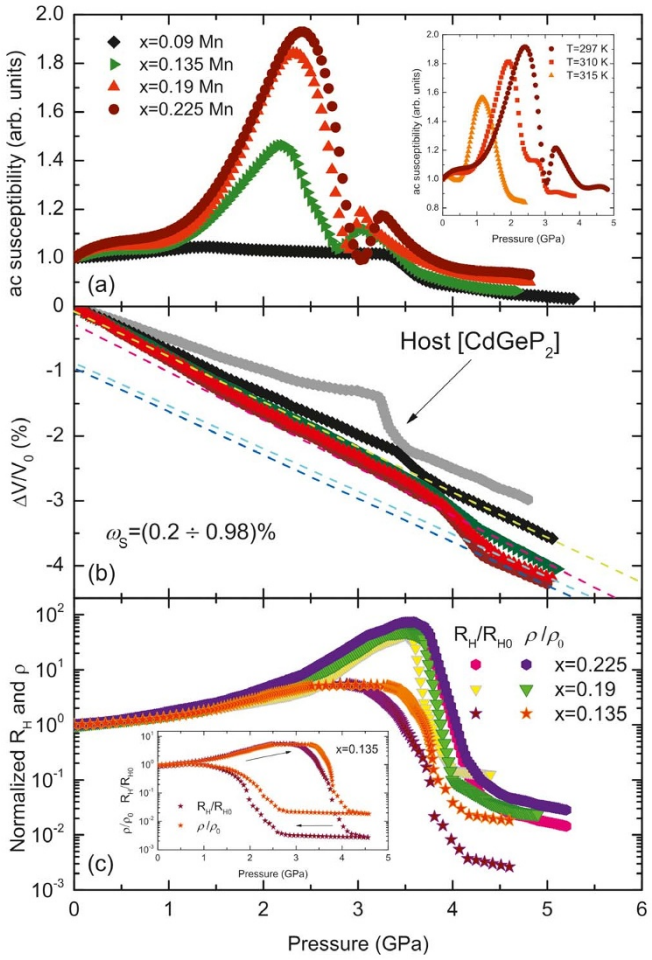

Figure 1 | High-pressure physical properties of $Cd_{1-x}Mn_xGeP_2$. (a) Magnetic ac susceptibility χ_{ac} as function of pressure for $0.09 \geq x \geq 0.225$ are obtained for $T = 300$ K. Inset shows selected χ_{ac} vs P at the temperature changes between RT and T_C (332 K) for $x = 0.225$. Note that χ_{ac} in the $CdGeP_2$ host does not develop any peak with pressure. (b) Relative volume $\Delta V(P)/V_0$ vs P measured at RT. Dashed lines show the extrapolation to $\Delta V(P)/V_0$ from high to zero pressure to evaluate ω_s. (c) resistivity ρ/ρ_0 and Hall coefficient R_H/R_{H0} vs P normalized to ambient pressure values for $0.135 \geq x \geq 0.225$. The absolute values at ambient pressure: $\rho = 2.75$, 3.02, 2, 0.72, 1530 Ω·cm and $R_H = 73.1$, 20, 10, 3, 5000 $cm^3 \cdot C^{-1}$ for $x = 0$, 0.09, 0.135, 0.19, and 0.225, respectively. A giant hysteresis is observed during decompression for $x = 0.135$ (inset).

Results

Magnetic ac-susceptibility. First of all, RT pressure dependence of the magnetic ac-susceptibility χ_{ac} for synthetized $Cd_{1-x}Mn_xGeP_2$ samples ($0.09 \geq x \geq 0.225$) was measured. At the studied pressure range (0–5.5 GPa), two bordered peaks, at $P_{C1} = 2.18$–2.4 GPa and at P_{C2} around 3 GPa, for $0.09 \geq x \geq 0.225$), were noted (Fig. 1a). The first peak in χ_{ac} as function of composition show remarkable upturn as the Mn doping concentration increases, with a red shift towards high pressures (see also Fig. S2 in the supplement material). This observation clearly marks up a magnetic transition from FM to NM state, which is largely leaded by the MnP clusters. At the end of this pressure interval, the ac-susceptibility goes back to the state of low pressure. At pressures close to 3 GPa, a second less intensive peak develops, showing a second transition with similar magnetic characteristics as the previous one. When doping concentration is low (for $x = 0.09$), the peak of χ_{ac} is negligible, suggesting very weak cluster correlation. Interestingly, both peaks happen to be very sensitive to changes in the temperature range between RT and T_C. Inset of Figure 1a displays how the first peak, for $x = 0.225$, is suppressed gradually while the second disappear completely when temperature is increased up to $T = 315$ K.

Volumetric and transport properties. Now we focus on the less intense second peak at P_{C2}, which happens around 3 GPa. Consistent *in situ* volumetric and transport high-pressure measurements performed at RT (Fig. 1b, c) reveal a new unexpected behavior. For example, an abrupt change in the pressure-dependent relative volume $\Delta V(P)/V_0$ (Fig. 1b) happens to be quite similar to that reported for $Cd_{1-x}Mn_xGeAs_2$[22], as well as for Invar-like bulk materials[23,24]. Furthermore, a large value of the spontaneous volume magnetostriction of $\omega_s = 0.2 \div 0.98\%$ for $x = 0.09 \geq x \geq 0.225$ was obtained from the extrapolation from the high to low-pressure regime, similarly to previous results[22]. This onset of ω_s exposes the rapid destabilization of the FM state under pressure that is related to the lattice compressibility and increase of the bulk moduli (see Fig. S3 in the Supplement material). Whereas the abrupt change in the slope around $P \approx 3.2$ GPa in the host sample is related to a structural phase transition driven by pressure. This topic will be further discussed with the help of *ab initio* calculations.

The discussed trend is clearly reflected in the performed transport measurements. In the host, for low doping Mn concentration ($x < 0.09$), there are only small changes in the samples resistivity ρ and the Hall coefficient R_H up to 3 GPa[21], see Fig. 1c. In contrast, we found more dramatic changes (between 3–4 orders of magnitude) in the values of $\rho(P)$ and $R_H(P)$ for larger doping concentrations. In particular for $0.135 \geq x \geq 0.225$ samples, a slightly upper P_{C2} was found (Fig. 1c), which is a typical characteristic of an insulator-metal transition[25]. The measured R_H in all cases specifies that charge carrier and keep with the same sign with pressure (even in a logarithmic normalized scale). The inset in Figure 1c displays a giant hysteresis which appear during decompression on both transport parameters for the $x = 0.135$ sample. We stress that this hysteretic behavior emerges only at higher Mn doping concentration ($0.135 \geq x \geq 0.225$). Based on all our measurements, we can suggest that the 3 GPa observed feature corresponds to a second transition from a FM to a NM state.

High-pressure zero-field magnetization. In order to ensure that both transitions are in fact originated from a two serial FM to NM states and their cluster dependences; we provide RT zero-field (ZF) magnetization measurements as function of pressure. In Fig. 2a,

unusual step-like behavior of ZF magnetization for $x = 0.225$ demonstrates two areas located at $P_{C1} = 2.4$ GPa and $P_{C2} = 3.3$ GPa evidencing well defined consecutive pressure-induced transitions. Both of these values are in well agreement the obtained peaks in χ_{ac} (Fig. 1a). Within the considered measured pressure range the total decrease in ZF magnetization is not exceeded by 10% and does not go to zero as expected for a cluster embedded in a crystal host[8]. For more accurate evolution of the magnetic behavior, we measured hysteresis loops at very weak magnetic fields, up to 1000 Am^{-1} (i.e. maximally achievable by coils). As depicted in Fig. 2b, the hysteresis characteristics of FM state for $x = 0.225$ starting from ambient up to 2.20 GPa and appearing again at 2.75 GPa (inset of Figure 2b) is clearly demonstrated.

DFT calculations. In order to strength our observations we now rely on DFT calculations, as implemented in the Vienna *ab initio* simulation package (VASP)[26] (see Methods, Computational details). Due to the fact that the experimentally measured MnP clusters are embedded in a crystalline system and they are not free, we have tried to understand its magnetic properties by studying the effect of the magnetic configuration changes in the crystalline system as a function of hydrostatic pressure, as well as on the substituted Mn atoms on the Cd vacancy[16] of the host. All calculated results are summarized in Fig. 3. Besides, we have studied the structural behavior of $CdGeP_2$ under pressure in order to elucidate the volumetric changes of Fig. 1b. Since the understanding of $CdGeP_2$ is the first step to elucidate the pressure behavior of $Cd_{1-x}Mn_xGeP_2$.

Figure 3a shows total energy calculation as function of volume for MnP crystalline cell. The crystallized cell with *Pnma* structure was created starting from the experimental values, as in Reference 27. Several MnP spin configurations were considered: NM, FM-I, FM-II, and FM-III, which are obtained by pressurizing the initial FM-I configuration. Here the FM configurations have the magnetic moment from 1.50, 1.20, and 0.53 μ_B/f.u. for FM-I, FM-II, and FM-III states, respectively. Our theoretical results indicate that the FM-I state corresponds to the lowest energy configuration. We then calculate the enthalpy difference ΔH as function of pressure at $T = 0$ K (Fig. 3b). The volume changes show three sharp consecutive steps FM-I → FM-II → FM-III at 5.5 GPa and 7.2 GPa (see Fig. S4 in the Supplement Material). In detail, this picture can be related to pressure-depended changes in the interatomic bond distances d along Mn-Mn (Fig. 3c) and Mn-P (Fig. 3d) atoms. This analysis stresses how the pressure is switching between different FM configurations (however, slightly overestimated experimental results), suggesting then isostructural transformations occurring in the cation coordination of the structure with *Pnma* space group, without involving group-subgroup structural changes. The transition between a magnetic and non-magnetic state is obtained around 9 GPa (depending on the used functional), a lower phase transition pressure can be obtained if the total free energy is used by considering vibrational contribution obtained from the quasi-harmonic approximation.

The theoretical results for the atomic Mn substitution in the host provide us additional confirmation that host-doping concentration leads to host structure stability under pressure, only if the role of pressure-induced decomposition and other possible high-pressure phases beyond the chalcopyrite type structure are excluded. This dependence shows no phase transitions up to 20 GPa, as it evident from weak reduction in lattice parameters (Fig. 3e). Furthermore, for both 0.125 mol% ($x = 0.005$) and 0.25 mol% ($x = 0.01$) Mn concentrations, we found a magnetic moment of 3.88 μ_B/Mn at ambient pressure that is then completely depleted around 20 GPa (Fig. 3f).

Figure 1b shows that $CdGeP_2$ and $Cd_{1-x}Mn_xGeP_2$ undergo a phase transition between 3 and 4 GPa, which is accompanied by a volume reduction, i.e. a first order phase transition. In order to consider possible structural phase transitions, we study the stability of $CdGeP_2$ by considering several structures reported as high-pressure phases of another chalcopyrite-type compounds. Among those, we put special attention on the modified NaCl-type cubic phase with P atoms on (0.25, 0.25, 0.25) position[28], and the NaCl-type structure with atoms located on a random distribution[29]. Our results do not show any phase transition to these phases below 10 GPa. However, it was observed that $CdGeP_2$ is decomposed into several compounds as pressure increases (see Fig. S4 from supplement material). Which could suggest that $Cd_{1-x}Mn_xGeP_2$ could experience decomposition under pressure, or a phase transition to a NaCl-type structure at pressures much higher than those investigated in this report. Nevertheless the identification of the high pressure phase will be addressed with future experiments.

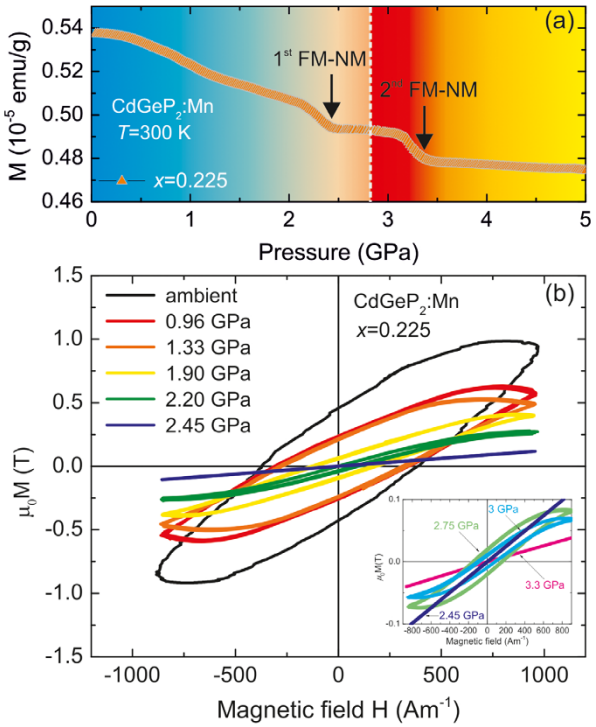

Figure 2 | High-pressure magnetic measurements. (a) ZF magnetization for $x = 0.225$ as function of applied pressure. Dashed line corresponds for appearance of second FM state as it further obtained from minor hysteresis loops vs magnetic field measured at pressures up to 2.45 GPa (b) and up to 3.3 GPa (inset). All measurements were performed at RT regime.

Discussion

Therefore, our data demonstrates a large magnetic dependence of the sample as function of pressure with large doping concentration. This is due to the presence of MnP clusters, which are strongly inhomogeneous in $Cd_{1-x}Mn_xGeP_2$. We do not observe any noticeable precipitation that indicates compound segregation for the pressure regimes considered. However, it is unclear how the FM clusters can be influenced by other inhomogeneous NM inclusions. Based on the EDS and SEM investigations, we can identify six different phases, including MnP clusters (70 μm approx.), all present at ambient conditions as noted in Fig. 4a and supplemental material. The presence of Mn could make the sample quite magnetic but our samples show mostly the formation of MnP clusters. Therefore, the effect of only Mn is largely reduced. Even in the case of host Mn substitutions, we find those to be in very low concentration and in general they cannot be attained as responsible for the intrinsic ferromagnetism. One point to have in consideration is that when pressure is applied (Figure 4b), the inhomogeneous phases observed in our samples of $Cd_{1-x}Mn_xGeP_2$ could separate and react as new subpro-

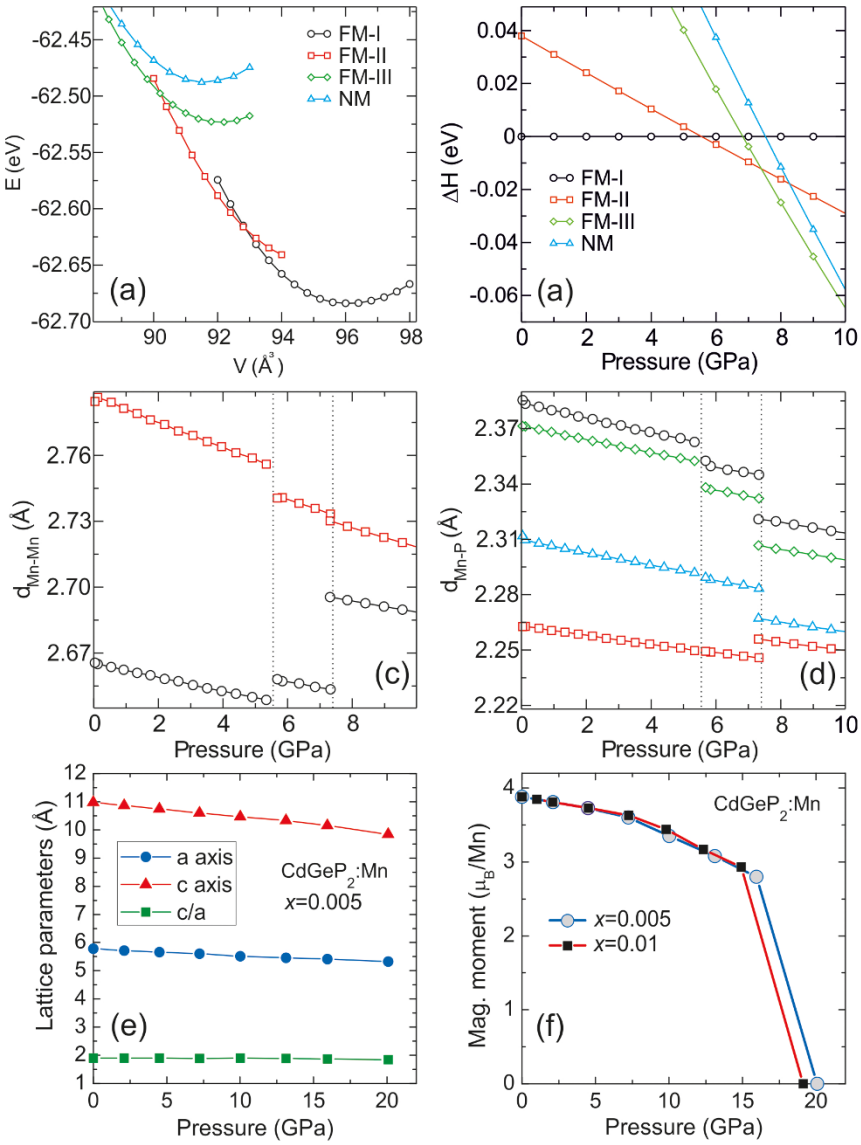

Figure 3 | Summarized DFT calculations for MnP clusters and substituted Mn atoms in $Cd_{1-x}Mn_xGeP_2$. (a) Total energy-volume curves for MnP clusters for non-magnetic (NM) and several FM spin configurations. (b) Enthalpy difference ΔH at $T = 0$ K as function of pressure for these configurations. The pressure dependence of Mn-Mn and Mn-P interatomic bond distances of MnP are presented in (c), and (d), respectively. Here dashed lines correspond to isostructural transformations in MnP at ≈5.5 GPa and 7.2 GPa. (f) Pressure evolution of lattice parameters and (g) magnetic moment at the specified Mn content when Mn atoms substituted in the host.

ducts due to the strong pressure-induced decomposition trend. However, this topic should be detailed studied in future experiments.

Next, we briefly comment on the implementation of pressure control of ferromagnetically ordered clusters. Recently, progress in the field of microfluidic technology has proposed to create a static digital control logic using pressure-gain valves[30]. Rendering this concept into the development of devices based on embedded magnetic clusters, it is possible to imagine that by controlling the cluster size in ferromagnetic chalcopyrites, could be possible then by pressure to manipulate the magnetic and electric response.

In summary, unconventional behavior of ferromagnetically MnP clusters in strongly inhomogeneous Mn-doped $CdGeP_2$ was investigated via effect of hydrostatic pressure and *ab initio* simulations. We find two serial transitions from FM to NM states at RT, which directly arises from cluster magnetic transitions (magnetic switching). Although, the detail microscopic physics of these phenomena was not completely addressed, future experimental and theoretical efforts should focused in those aspects. Even though, the results here

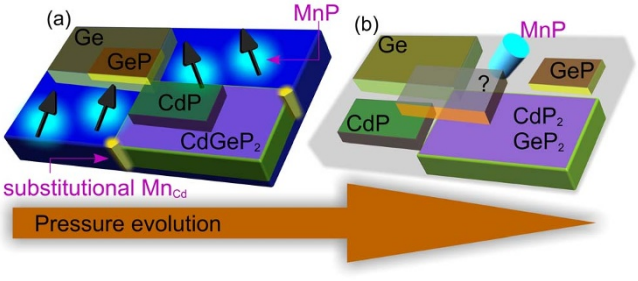

Figure 4 | A schematic illustration of strongly inhomogeneous $Cd_{1-x}Mn_xGeP_2$ with MnP clusters and substituted Mn atoms in the host. (a) There are six different phases, including MnP clusters at normal conditions. (b) When pressure in applied there is possible separation and appears of new subproducts due to pressure-induced decomposition trend.

discussed present a pressure controlled mechanism that affect directly on the clusters magnetization. This novel scenario of using Mn-doped chalcopyrites in fabrication devices based on the micro-fluidic control via pressure-gain[28] is a path worth of pursuing.

Methods

Samples. Polycrystalline samples of $Cd_{1-x}Mn_xGeP_2$ with $0 \geq x \geq 0.225$ were prepared by the direct fusion method. The procedure of synthesis, as well as magnetization data at ambient pressure is presented elsewhere[31]. In this work, we focus on Mn concentration of $x = 0.225$, where the obtained T_C was 332 K, to our knowledge the highest value for this compound[20]. All samples $Cd_{1-x}Mn_xGeP_2$ with $0 \geq x \geq 0.225$ were characterized by high-resolution x-ray diffraction (HRXRD), EDS and SEM. According to HRXRD data, the main crystal phase was identified as the tetragonal chalcopyrite structure $CdGeP_2$ with space group *I*42*d*. The EDS and SEM analysis point to inhomogeneous distribution of several phases, including magnetically MnP clusters on the micron size. The detailed description of sample characterization can be found in the Supplementary material (see Fig. S1).

High-pressure measurements. *In situ* volumetric and transport measurements were performed in *Toroid* type high-pressure apparatus by combination of high-precision strain gauge technique and a six-probe method on samples of $3 \times 1 \times 1$ mm3 in size (see References 32 and 33 for details). High-pressure ac-susceptibility and ZF magnetization measurements were implemented by conventional self-excited frequency and inductance methods respectively. A pure mixture of ethanol-methanol 4 : 1 was used as a pressure-transmitting medium. Pressure inside the teflon cell with useful volume ≈80 mm^3 was continuously monitored by a manganin wire and calibrated on the end points to the Bi phase transition.

Computational details for MnP crystals. Total energy calculations and structural optimizations were performed within the framework of the density functional theory (DFT) and the projector-augmented wave (PAW)[34,35] method as is implemented in the Vienna *ab initio* simulation package (VASP)[26,36]. We use a plane-wave energy cutoff of 356 eV to ensure a high precision in all our calculations. The GGA of Perdew, Burke and Ernzerhof (PBE)[37] based on the projector augmented wave (PAW)[34] method was used to treat the exchange-correlation (XC) functional. Monkhorst-Pack scheme was employed to discretize the Brillouin-zone (BZ) integrations[38] with a mesh of $4 \times 5 \times 4$ for MnP crystal. In the relaxed equilibrium configuration, the forces are less than 3 meV/Å per atom in each of the Cartesian directions. We have used the antiferromagnetic (AFM, Mn: ↑↑↓↓, ↑↓↑↓, ↑↓↓↑), ferromagnetic (FM, Mn: ↑↑↑↑) and nonmagnetic (NM) configurations for MnP. According to our results the AFM phases are energetically noncompetitive against the FM and NM phases for MnP.

Computational details for Mn substitutional atoms. We have initiated our calculations, by taking the *I*42d crystal structure of $CdGeP_2$, consisting of 16 atoms (Cd = 4 atoms, Ge = 4 atoms and P = 8 atoms) in the unit cell. To dope with 0.125% and 0.25% of Mn atoms, we have constructed the $2 \times 2 \times 1$ and $2 \times 1 \times 1$ supercells of $CdGeP_2$, respectively. The energy cutoff of 600 eV for plane wave basis and $8 \times 8 \times 8$ *K*-point mesh, generated by Gamma method for Brillouin zone sampling, were found suitable to ensure the sufficient convergence, until the Hellman-Feyman forces acting on each atom became less than 0.005 eV/Å.

1. Sinova, J. & Zutic, I. New moves of the spintronics tango. *Nature Materials* **11**, 368–371 (2012).
2. Pesin, D. & MacDonald, A. H. Spintronics and pseudospintronics in graphene and topological insulators. *Nature Materials* **11**, 409–416 (2012).
3. Bauer, G. E. W., Saitoh, E. & van Wees, B. J. Spin caloritronics. *Nature Mater.* **11**, 391–399 (2012).
4. Wakamura, T., Hasegawa, N., Ohnishi, K., Niimi, Y. & Otani, Y. Spin injection into a superconductor with strong spin-orbit coupling. *Phys. Rev. Lett.* **112**, 036602 (2014).
5. Torrejon, J. *et al.* Unidirectional thermal effects in current-induced domain wall motion. *Phys. Rev. Lett.* **109**, 106601 (2012).
6. Piano, S. *et al.* Spin polarization of (Ga,Mn)As measured by Andreev spectroscopy: the role of spin-active scattering. *Phys. Rev. B* **83**, 081305(R) (2011).
7. Binh, D. Le. *et al.* Europium Nitride: a novel diluted magnetic semiconductor. *Phys. Rev. Lett.* **111**, 167206 (2013).
8. Jamet, M. *et al.* High-Curie-temperature ferromagnetism in self-organized $Ge_{1-x}Mn_x$ nanocolumns. *Nature Mater.* **5**, 653–659 (2006).
9. Hynninen, T., Raebiger, H., von Boehm, J. & Ayuela, A. High Curie temperatures in (Ga,Mn)N from Mn clustering. *Appl. Phys. Lett.* **88**, 122501 (2006).
10. Zhang, S. X. *et al.* Magnetism and anomalous Hall effect in Co-(La,Sr)TiO_3. *Phys. Rev. B* **76**, 085323 (2007).
11. Dung, D. D. & Cho, S. Anomalous Hall effect in epitaxially grown ferromagnetic FeGa/Fe_3Ga hybrid structure: evidence of spin carrier polarized by clusters. *J. Appl. Phys.* **113**, 17C734 (2013).
12. Kilanski, L. *et al.* Colossal linear magnetoresistance in a $CdGeAs_2$:MnAs micro-composite ferromagnet. *Solid State Commun.* **151**, 870 (2011).
13. Aitken, J. A., Tsoi, G. M., Wenger, L. E. & Brock, S. L. Phase segregation of MnP in chalcopyrite dilute magnetic semiconductors: a cautionary tale. *Chem. Mater.* **19**, 5272–5278 (2007).
14. Hwang, T., Shim, J. H. & Lee, S. Observation of MnP magnetic clusters in room-temperature ferromagnetic semiconductor $Zn_{1-x}Mn_xGeP_2$ using nuclear magnetic resonance. *Appl. Phys. Lett.* **83**, 1809 (2003).
15. Erwin, S. C. & Zutic, I. Tailoring ferromagnetic chalcopyrites. *Nature Mater.* **3**, 410–414 (2004)
16. Mahadevan, P. & Zunger, A. Room-temperature ferromagnetism in Mn-doped semiconducting $CdGeP_2$. *Phys. Rev. Lett.* **88**, 047205 (2002).
17. Cho, S. *et al.* Room-Temperature Ferromagnetism in $(Zn_{1-x}Mn_x)GeP_2$ semiconductors. *Phys. Rev. Lett.* **88**, 257203 (2002).
18. Zhao, Y.-J., Geng, W. T., Freeman, A. J. & Oguchi, T. Magnetism of chalcopyrite semiconductors: $Cd_{1-x}Mn_xGeP_2$. *Phys. Rev. B* **63**, 201202(R) (2001).
19. Arslanov, T. R. *et al.* Emergence of pressure-induced metamagnetic-like state in Mn-doped $CdGeAs_2$ chalcopyrite. *Appl. Phys. Lett.* **103**, 192403 (2013).
20. Medvedkin, G. A. I. *et al.* Room Temperature Ferromagnetism in Novel Diluted Magnetic Semiconductor $Cd_{1-x}Mn_xGeP_2$. *Jpn. J. Appl. Phys.* **39**, L949 (2000).
21. Mollaev, A. Yu. *et al.* Phase transition in multicomponent semiconductor $Cd_{1-x}Mn_xGeP_2$ under hydrostatic pressure up to 7 GPa. *High Press. Res.* **26**, 387 (2006).
22. Mollaev, A. Yu. *et al.* Anomalies of magnetic properties and magnetovolume effect in $Cd_{1-x}Mn_xGeAs_2$ at hydrostatic pressure. *Appl. Phys. Lett.* **100**, 202403 (2012).
23. Winterrose, M. L. *et al.* Pressure-Induced Invar Behavior in Pd_3Fe. *Phys. Rev. Lett.* **102**, 237202 (2009).
24. Sidorov, V. & Khvostantsev, L. Magnetovolume effects and magnetic transitions in the invar systems $Fe_{65}Ni_{35}$ and $Er_2Fe_{14}B$ at high hydrostatic pressure. *J. Mag. Mag. Mat.* **129**, 356–360 (1994).
25. Satya, A. T. *et al.* Pressure-induced metallization of $BaMn_2As_2$. *Phys. Rev. B* **84**, 180515(R) (2011).
26. Kresse, G. & Furthmüller, J. Efficient iterative schemes for *ab initio* total-energy calculations using a plane-wave basis set. *Phys. Rev. B* **54**, 11169 (1996).
27. Gercsi, Z. & Sandeman, K. G. Structurally driven metamagnetism in MnP and related *Pnma* compounds. *Phys. Rev. B* **81**, 224426 (2010).
28. Abdellaoui, A., Ghaffour, M., Bouslama, M., Benalia, S., Ouerdane, A. *et al.* Structural phase transition, elastic properties and electronic properties of chalcopyrite $CuAlX_2$ (X = S, Se, Te). *J. Alloys Comp.* **487**, 206 (2009).
29. Beister, H. J., Ves, S., Hönle, W., Syassen, K. & Kühn, G. Structural phase transitions and optical absorption of $LiInSe_2$ under pressure. *Phys. Rev. B* **43**, 9635 (1991).
30. Weaver, J. A., Melin, J., Stark, D., Quake, S. R. & Horowitz, M. A. Static control logic for microfluidic devices using pressure-gain valves. *Nature Phys.* **6**, 218–223 (2010).
31. Novotortsev, V. M. *et al.* Ferromagnetic material $CdGeP_2$:Mn for spintronics. *Russian J. Inorg. Chem.* **51**, 1153–1156 (2006).
32. Khvostantsev, L. G., Slesarev, V. N. & Brazhkin, V. V. Toroid type high-pressure device: history and prospects. *High Press. Res.* **24**, 371–383 (2004).
33. Yel'kin, F. S., Tsiok, O. B. & Khvostantsev, L. G. The strain gauge technique for measuring the compressibility of solids at high pressures and temperatures. *Instrum. Exp. Tech.* **46**, 101–107 (2003).
34. Blöchl, P. E. Projector augmented-wave method. *Phys. Rev. B* **50**, 17953 (1994).
35. Kresse, G. & Joubert, D. From ultrasoft pseudopotentials to the projector augmented-wave method. *Phys. Rev. B* **59**, 1758 (1999).
36. Kresse, G. & Furthmüller, J. Efficiency of *ab-initio* total energy calculations for metals and semiconductors using a plane-wave basis set. *J. Comput. Mat. Sci.* **6**, 15–50 (1996).
37. Perdew, J. P., Burke, K. & Ernzerhof, M. Generalized gradient approximation made simple. *Phys. Rev. Lett.* **77**, 3865 (1996).
38. Monkhorst, H. J. & Pack, J. D. Special points for Brillouin-zone integrations. *Phys. Rev. B* **13**, 5188 (1976).

Acknowledgments

We thank V.V. Brazhkin and I.O. Troyanchuk for valuable discussions. This work was supported by the RAS Presidium Program N.37 "Physics of High Pressure", partly financed from funds for science in 2011–2014, under the Project No. N202 166840 granted by the National Center for Science of Poland. We also would like to acknowledge Swedish Energy Agency (STEM) and Carl Trygress Foundation by Swedish Institute (SI) for financial support. M. R. acknowledges the support from Higher Education Commission (HEC) of Pakistan. SNIC and UPPMAX have provided computing time for this project. AHR recognizes the support of the Marie Curie Actions from the European Union in the international incoming fellowships (grant PIIFR-GA-2011-911070). S.L.-M. and A.H.R. acknowledge the computer resources provided by RES (Red Española de Supercomputación), the TACC-Texas supercomputer center and MALTA-Cluster. S.L.-M. has been supported by CONACyT México under the program of CATEDRAS for young researchers.

Author contributions

R.K.A. conceived and designed the experiments. V.M.T., T.V.S. and S.F.M. grew the samples. L.K., R.M. and A.R. performed characterization of samples. S.L.-M., A.H.R., M.R.,

P.P. and R.A. carried out DTF calculations. R.K.A. and T.R.A. performed high-pressure measurements, and data analysis. T.R.A. wrote the manuscript with reviews and inputs from R.A., A.H.R. and T.C. A.Y.M. and I.K.K. supervised the project. All authors contributed to discussions.

Additional information

Supplementary information accompanies this paper at http://www.nature.com/scientificreports

Competing financial interests: The authors declare no competing financial interests.

How to cite this article: Arslanov, T.R. *et al.* Pressure control of magnetic clusters in strongly inhomogeneous ferromagnetic chalcopyrites. *Sci. Rep.* **5**, 7720; DOI:10.1038/srep07720 (2015).